The diatomic dication SiC^{2+} in the gas phase

Reinaldo Pis Diez[a], Julio A. Alonso[b,c]

[a]*Departamento de Química, CEQUINOR, Centro de Química Inorgánica (CONICET, UNLP), Facultad de Ciencias Exactas, UNLP, CC 962, 1900 La Plata, Argentina.*
[b]*Departamento de Física Teórica, Atómica y Optica, Universidad de Valladolid, E-47011 Valladolid, Spain.*
[c]*Donostia International Physics Center, 20080 San Sebastian, Spain.*

Abstract

The diatomic dication SiC^{2+} in the gas phase is studied using the state-averaged version of the CASSCF method and the state-specific MRMP perturbation theory to recover dynamical correlation effects. Thirteen different electronic states of the dication were found and characterized, ten of them being metastable electronic states. The ground state is characterized by a $^3\Pi$ electronic state. The leading configuration state functions are provided for each electronic state. For completeness, a similar study is presented both for SiC and for SiC$^+$. The present results are in excellent agreement with results obtained by other authors. The adiabatic ionization energies of SiC$^+$ to form SiC^{2+} are within a range from about 16 eV to about 19.5 eV. This finding indicates that a projectile, whose ionization energy lies within that range could be eventually used to produce the dication. Lifetimes and radiative transition dipole moments are also calculated and reported.

Keywords: SiC^{2+}, SA-CASSF, MRMP2

1. Introduction

Small molecules formed by silicon and carbon, as the simple neutral SiC molecule, have been identified in astrophysical environments several years ago. [1, 2] The first experimental observation of SiC in the gas phase was performed in 1988 by Bernath et al., [3] whereas the first theoretical study of that species dates from 1974 when Lutz and Ryan carried out a series of

---

configuration interaction calculations on the three lowest-energy electronic states of SiC. [4] In spite of several theoretical studies performed on neutral SiC after the work of Lutz and Ryan, the recent works of Borin and coworkers, [5] Pramanik and Das, [6] and Shi et al. [7] seem to present the more exhaustive studies on a variety of low-lying electronic states of SiC. In the first case and in the latter case the complete active space self-consistent field (CASSCF) methodology was used to deal with the static correlation problem. The state-averaged version of CASSCF, known as SA-CASSCF, was used by Borin et al. Dynamical correlation effects were taken into account by means of the internally contracted multi-reference configuration interaction (IC-MRCI) method. Correlation consistent cc-pV5Z and aug-cc-pV6Z basis sets were used in those works. Pramanik and Das, on the other hand, utilized the multi-reference configuration interaction method, including single and double excitations (MRCISD) with relativistic core potentials and specially designed valence basis sets. The potential energy curves of about twenty-five electronic states of SiC, including singlets, triplets and quintets, were reported by those authors, with emphasis not only on geometric and electronic properties but also on spectroscopic constants.

Very recently, too, Pramanik and coworkers calculated the electronic states and spectroscopic properties of SiC^+ using large scale calculations within the context of the MRDCI method and the same type of core potentials and basis sets described in the previous paragraph. [8] The potential energy curves of fourteen electronic states of SiC^+, including doublets and quartets, were reported by those authors, with emphasis on geometric, electronic and spectroscopic features. Moreover, those authors provide a good overview of previous theoretical works on SiC^+, emphasizing that no experimental information is available for that species.

The diatomic dication SiC^{2+} was first observed in the gas phase in 1978 by Nakamura and Kuroda, who used atom probe mass spectrometry with a silicon carbide tip. [9] These findings were recently confirmed by Tang et al. using essentially the same technique for Ti-Si-N hard-coatings containing C impurities. [10] In addition, SiC^{2+} was also observed with two other mass spectrometric methods, namely by Dietze et al. using spark-source mass spectrometry [11] and recently by Franzreb and Williams by means of oxygen ion beam sputtering of silicon carbide in a secondary ion mass spectrometry instrument. [12] The experimental finding of Franzreb and Williams was mentioned in the supplementary material (available online) of ref. [13] but data were not shown. Their mass spectra of SiC^{2+} are shown in the sup-

plementary material of the present work for the first time. The experimental identification of SiC^{2+} is also discussed.

On the other hand, no detailed theoretical studies exist for SiC^{2+}, even though an early preliminary effort to perform semiempirical calculations on SiC^{2+} was made by Dietze et al. [11] In the present work, an exhaustive study of various electronic states of SiC^{2+}, including singlets, triplets and quintets, is carried out within the context of the SA-CASSCF method to deal with static correlation effects and the state-specific multireference Møller–Plesset perturbation theory (MRMP2) for dynamical correlation effects. For completeness, the lowest-energy electronic states of neutral SiC and monocation SiC^+ are also calculated and compared with experimental and theoretical results of other authors.

2. Calculation details

The MCSCF part of the calculations was carried out by means of the state-averaged version of the complete active space self-consistent field (SA-CASSCF) method. [14, 15] The graphical unitary group approach [16, 17] (GUGA) was used to solve the CI problem. The active space was formed by the 2s and 2p C atomic orbitals (AO) and the 3s and 3p Si AOs, that is, eight electrons in eight orbitals. The 1s C AO and the 1s, 2s and 2p Si AOs were kept frozen in the inactive space. Symmetry was exploited by means of the C_{2v} point group, and the different irreducible representations (IREP) of the group were used to label the configuration state functions (CSF) used in the GUGA. The aug-cc-pVTZ basis set was used both for C and Si. [18, 19]

For neutral SiC, 492, 408 and 432 CSFs were generated for the A_1, A_2 and $B_{1,2}$ IREPs, respectively, for the singlet electronic state. In the case of the triplet electronic state, 584, 584 and 592 CSFs were created for the A_1, A_2 and $B_{1,2}$ IREPs, respectively. Finally, 184, 184 and 176 CSFs were formed for the A_1, A_2 and $B_{1,2}$ IREPs, respectively, to study the quintet electronic state.

For SiC^+, 616, 560 and 588 CSFs were generated for the A_1, A_2 and $B_{1,2}$ IREPs, respectively, for the doublet electronic state. 320, 352 and 320 CSFs were formed for the A_1, A_2 and $B_{1,2}$ IREPs, respectively, for the quartet electronic state. To study the sextet electronic state, 60, 48 and 54 CSFs were considered for the A_1, A_2 and $B_{1,2}$ IREPs, respectively.

To investigate the singlet electronic state of SiC^{2+}, 328, 272 and 288 CSFs were generated for the A_1, A_2 and $B_{1,2}$ IREPs, respectively. 360, 384 and 384

CSFs were formed for the A_1, A_2 and $B_{1,2}$ IREPs, respectively, for the triplet electronic state, whereas the quintet electronic state was studied after 96, 116 and 104 CSFs for the A_1, A_2 and $B_{1,2}$ IREPs, respectively, were generated.

Three states were averaged for each IREP and for each electronic multiplicity of every diatomic species. In this way, the potential energy curves for 81 different electronic states for SiC, SiC^+ and SiC^{2+} were constructed between 1.60 and 10.0 Å. A grid containing 56 points was used to that end. The grid is far more dense around the equilibrium distances, whereas it becomes sparser when the atoms approach dissociation.

Dynamical correlation effects were introduced on the multireference wavefunctions by the state-specific multireference Møller–Plesset perturbation theory (MRMP2) developed by Hirao. [20, 21] MRMP2 calculations were carried out on the corresponding minima of the SA-CASSCF potential energy curves obtained as described in the previous paragraphs. When metastable states were achieved, as in SiC^+ and SiC^{2+}, MRMP2 calculations were also performed on the corresponding maxima or top of the energy barriers. The 1s C AO and the 1s, 2s and 2p Si AOs were kept frozen during the calculations. The aug-cc-pV5Z basis set was used in this case both for C and Si. [18, 19]

Equilibrium bond distances, harmonic vibrational frequencies and zero-point energies were estimated from the potential energy curves obtained at the SA-CASSCF/aug-cc-pVTZ level of theory, whereas dissociation energies and energy separations between states were calculated at the MRMP2/aug-cc-pV5Z level of theory. These two last quantities include the zero-point correction. Radiative transition dipole moments were also calculated. In this case, the aug-cc-pVQZ basis function was used due to software limitations.

All the calculations were performed with the GAMESS-US package. [22, 23] Equilibrium distances, harmonic vibrational frequencies and zero-point energies were derived from numerical fitting of the potential energy curves obtained at the SA-CASSCF/aug-cc-pVTZ level of theory to a quadratic function of the energy with respect to the interatomic distance.

Lifetimes were also calculated to gain insight into the possibility of experimental detection of the metastable states found. The simple, semiclassical WKB approximation [24] is used for this purpose. The lifetime is calculated as

$$\tau = \frac{1}{\nu T} \tag{1}$$

where ν is the dimer vibrational frequency in s^{-1}, and T is the transmission

coefficient, given by

$$T = \exp(-\frac{2}{\hbar} \int \{2m[V(r) - E]\}^{1/2} dr).$$

In the above equation m is the reduced mass of the diatomic molecule, $V(r)$ is the total potential energy as function of the internuclear distance r, and E is the energy evaluated at the lowest vibrational state. The integral is calculated between the classical turning points of the potential energy curve.

3. Results and discussion

Table 1 summarizes the results obtained in this work for the neutral SiC diatomic molecule. Moreover, a comparison with other experimental and theoretical results is provided in the table. The relative ordering of the first thirteen electronic states of SiC is well reproduced by the methodology used in the present work. The ground state of SiC is predicted to be $^3\Pi$, in accordance with other results, see Table 2 for the electronic configuration in terms of CSF for all reported states. The notation used for π orbitals, $\pi^2(\uparrow; \uparrow)$ for example, indicates the population of the two components of such orbitals, which are separated by a semicolon. The equilibrium distances obtained in this work are in general slightly larger than the values shown by other authors, although there is a good agreement with the values informed by Pramanik and Das, [6] which used the MRCISD method. Dissociation energies are in a very acceptable agreement with the ones reported by Borin et al. [5], with differences no larger than about 0.10 eV. The only exception is the e$^1\Sigma^-$ electronic state, for which a dissociation energy of 2.10 eV is informed in ref. 5, whereas a value of 1.32 eV is found in the present work. Harmonic vibrational frequencies obtained with the methodology used in this work lie within the range of frequencies calculated by other authors, although in various cases it is observed that they are smaller than the values shown in other works. The energy separations calculated in this work show the same behavior of the harmonic vibrational frequencies, that is, they lie within the range of calculated and experimental values, but they are smaller than values obtained by other authors in some selected cases. It is found, furthermore, that twelve electronic states of SiC correlate to the triplet electronic ground states of Si and C, the only exception being the E$^3\Pi$ state, which correlates to the Si (^{1}D) + C (^{3}P) states. These findings are in complete agreement with those reported by Borin et al. [5]

The results achieved for SiC$^+$ are shown in Table 3. It is seen from the table that the relative ordering of the first eight electronic states of the monocation found in the present work is in agreement with the ordering reported by Pramanik et al. [8] The electronic configurations in terms of CSF are shown in Table 4. The equilibrium distances agree very well with those shown by Pramanik et al., with discrepancies not larger than 0.04 Å. The exception is the b$^2\Pi$ state, for which an equilibrium distance of 1.748 Å is found in the present work, whereas a value of 1.99 Å was obtained in ref. 8. Harmonic vibrational frequencies are well described in general, with the larger differences with respect to those reported in ref. 8 being about 40 cm^{-1}. Exceptions are the d$^2\Sigma^+$ state, for which the discrepancy is as large as 80 cm^{-1}, and the b$^2\Pi$ one, for which two frequencies are provided in ref. 8. Dissociation energies can be compared for the two lowest-energy states only. It can be seen from the table that the present results are larger than the ones reported by Pramanik et al. by about 0.30-0.40 eV. Energy separations are very well described by the present methodology. Moreover, it is found that the D$^4\Pi$ state is a metastable state characterized by an appreciable energy barrier of 1.63 eV with respect to the dissociation limit and located at 2.261 Å. Interestingly, Pramanik et al. also found some metastable states for SiC$^+$, but those were not discussed. Finally, it is found that thirteen electronic states of SiC$^+$ correlate to Si$^+$ (^{2}P) + C (^{3}P) states. The only exceptions are the h$^2\Sigma^+$ state, which correlates to the Si$^+$ (^{2}P) + C (^{1}D) states and the 1$^6\Pi$ and 2$^6\Pi$ states, which are related to the Si$^+$ (^{4}P) + C (^{3}P) states. These findings are in agreement with those reported by Pramanik et al. [8]

The results reported in the two previous paragraphs indicate that the present methodology is sufficiently reliable to be used to describe the electronic states of SiC^{2+}.

Table 5 shows the results obtained for SiC^{2+}. Thirteen electronic states were found for the doubly charged molecule and their potential energy curves are shown in Figures 1 and 2. Ten states were found to be metastable states. The exceptions are the B$^3\Sigma^-$ and e$^1\Pi$ states, which are bound states with large equilibrium distances, see Table 5, and the 1$^5\Sigma^-$ state, which exhibits an energy barrier but the minimum is located below the dissociation limit, see Figure 1. Another interesting case is the C$^3\Pi$ state, which shows both a stable minimum at 4.415 Å and a metastable minimum that appears at 1.821 Å, see Figure 1. That behavior explains why the C$^3\Pi$ electronic state appears twice in Table 5. The ground metastable state of SiC^{2+} is found to be X$^3\Pi$, whereas three lowest-lying excited states lie 1 eV above the ground

state, namely, $a^1\Sigma^+$, $A^3\Sigma^-$ and $b^1\Pi$.

Calculated lifetimes are shown in Figures 1 and 2 for the metastable states found in the present work. It can be seen from the figures that the lifetimes of the $X^3\Pi$, $A^3\Sigma^-$, $2^5\Delta$, $3^5\Pi$, $a^1\Sigma^+$ and $c^1\Delta$ metastable states are virtually infinite, suggesting that they are good candidates to be experimentally detected. Interestingly, the lifetimes of the $X^3\Pi$ and $A^3\Sigma^-$ metastable states are equal to 1.24×10^{70} and 8.02×10^{70} seconds, respectively, when they are calculated from their own potential energy curves. However, a close inspection to the potential energy curves of the $X^3\Pi$, $A^3\Sigma^-$, $a^1\Sigma^+$ and $b^1\Pi$ metastable states clearly shows that the curves cross each other, see Figure 3. Although those crossings does not alter the dissociation channels of the $X^3\Pi$ and $A^3\Sigma^-$ metastable states, they offer dissociation paths with much lower lifetimes to those states, see Figure 1. The $C^3\Pi$, $b^1\Pi$, $f^1\Pi$ and $d^1\Sigma^+$ metastable states present lifetimes in the range from about 10^{-7} seconds to about 10^{-12} seconds, indicating that their experimental detection could be more difficult than in the previous cases.

It can be seen in Table 5 that the $a^1\Sigma^+$ and $b^1\Pi$ metastable states can be described by a leading CSF, whereas the $A^3\Sigma^-$ metastable state needs two CSFs for an adequate characterization. The $X^3\Pi$, $A^3\Sigma^-$, $a^1\Sigma^+$, $b^1\Pi$, $c^1\Delta$, $d^1\Sigma^+$ and $f^1\Pi$ states correlate to the Si^+ (^2P) + C^+ (^2P) atomic states. The $B^3\Sigma^-$ and $C^3\Pi$ correlate to the Si^{2+} (^1S) + C (^3P) states. The three $1^5\Sigma^-$, $2^5\Delta$ and $3^5\Pi$ quintet states correlate to the Si^+ (^4P) + C^+ (^2P) atomic states. Finally, the high-energy $e^1\Pi$ singlet states correlates to the Si^{2+} (^1S) + C (^1P) states. It is important to emphasize that the dissociation limit described by the Si^+ (^4P) + C^+ (^2P) atomic states is only 0.047 eV lower in energy than the Si^{2+} (^1S) + C (^3P) one at the MRMP2/aug-cc-pV5Z level of theory. Thus, the two asymptotes are almost indistinguishable for the scales shown in Figures 1 and 2.

Radiative transition dipole moments, in their length form, are shown in Table 6. The transition moments are calculated at the equilibrium distance of the lower-energy state involved in the transition. It is seen in the table that the transition moments can be divided into three groups. The first group presents transition dipole moments around or lower than 0.01 atomic units. The second one exhibits transition dipole moments between 0.2 and 0.1 atomic units. Finally, the third group contains only two transitions, which present large transition dipole moments. Those transitions are $b^1\Pi \to e^1\Pi$ and $X^3\Pi \to C^3\Pi$.

Table 7 summarizes the adiabatic ionization energies, AIE, of t lowest-

lying states of SiC and SiC$^+$. The present results are in excellent agreement with AIE reported by Pramanik et al. [8] The energy needed to create adiabatically the X$^4\Sigma^-$ ground state of SiC$^+$ from the ground state of neutral SiC is reported to be 8.76 eV by Pramanik et al., whereas the AIE relating those two states is found to be 8.80 eV in the present work. The second lowest-energy electronic state of SiC$^+$, the a$^2\Delta$, is reported to be 10.04 eV above the ground state of SiC by Pramanik et al., [8] whereas the AIE calculated in the present work is 9.97 eV. The c$^2\Sigma^-$ electronic state of SiC$^+$ is reported to be 10.17 eV above the ground state of SiC, [8] whereas the same state of the monocation is found to be 10.16 eV above the ground state of neutral SiC according to present methodology. Besides those results, Table 7 shows also the AIE of some low-lying electronic states of neutral SiC, like A$^3\Sigma^-$, a$^1\Sigma^+$, b$^1\Pi$, c$^1\Delta$, and 1$^5\Pi$. Moreover, the table shows the AIE of SiC$^+$, relating the lowest-lying electronic states of the monocation to the lowest-lying ones of SiC^{2+}. Interestingly, the AIE2 involving the ground states of both SiC$^+$ and SiC^{2+} is found to be 17.42 eV. Table 6 summarizes thirteen different AIE2, which lie within the range from about 16 to about 19.50 eV. Those values suggest that SiC^{2+} could be created from SiC$^+$ by simple reactions like SiC$^+$ + X$^+$ → SiC^{2+} + X or SiC$^+$ + X^{2+} → SiC^{2+} + X$^+$, in which the species X and X$^+$ present ionization energies within the range of the AIE of SiC$^+$. Some few examples are F, Be$^+$, Al$^+$ and As$^+$, for which the ionization energies are 17.42, 18.21, 18.83 and 18.59 eV, respectively. [25]

4. Conclusions

The diatomic dication SiC^{2+} in the gas phase was studied from a theoretical point of view using the state-averaged version of the complete active space self-consistent field and the state-specific multireference Møller–Plesset perturbation theory. Thirteen different electronic states of the dication were characterized, ten of them being metastable electronic states. The ground state is characterized by a $^3\Pi$ electronic state. Two other electronic states exhibit a minimum without any energy barrier, but they are higher in energy with respect to the ground state of SiC^{2+}. Another triplet state presents two minima, one of them, very shallow, appearing before the energy barrier, whereas the second minimum describes a metastable state for that triplet state. The leading configuration state functions are provided for each electronic state.

Calculated lifetimes indicate that most of the metastable states could

be experimentally detected. Moreover, large radiative transition dipole moments are observed between some metastable states of Π symmetry.

The adiabatic ionization energies of SiC^+ to form the dication are within a range from about 16 eV to about 19.5 eV. This fact indicates that a projectile with a ionization energy within that range could be eventually used to produce the dication from the monocation. Some examples are provided.

For completeness, a similar study is presented both for SiC and for SiC^+. The present results are in excellent agreement with results obtained by other authors.

Acknowledgment

References

[1] A. Suzuki, Prog. Theor. Phys. 62 (1979) 936.

[2] J. Cernicharo, C. Gottlieb, M. Guelin, P. Thaddeus, J. Vrtilek, Astrophys. J. Lett. 341 (1989) L25.

[3] P. F. Bernath, S. A. Rogers, L. C. OBrien, C. R. Brazier, A. D. McLean, Phys. Rev. Lett. 60 (1988) 197.

[4] B. L. Lutz, J. A. Ryan, Astrophys. J. 194 (1974) 753.

[5] A. C. Borin, J. P. Gobbo, R. de Souza Batista, L. G. M. de Macedo, Chem. Phys. 312 (2005) 213.

[6] A. Pramanik, K. K. Das, J. Mol. Spectrosc. 244 (2007) 13.

[7] D. H. Shi, W. Xing, J. F. Sun, Z. L. Zhu, Eur. Phys. J. D 66 (2012) 262.

[8] A. Pramanik, S. Chakrabarti, K. K. Das, Chem. Phys. Lett. 450 (2008) 221.

[9] S. Nakamura, T. Kuroda, Surf. Sci. 70 (1978) 452.

[10] F. Tang, B. Gault, S. P. Ringer, P. Martin, A. Bendavid, J. M. Cairney, Scripta Mater. 63 (2010) 192.

[11] H.-J. Dietze, S. Becker, P. Franke, C. Weiss, J. Reinhold, Isot. Environ. Healt. S. 20 (1984) 281.

[12] K. Franzreb, P. Williams, Arizona state university, 2007. Unpublished experimental results.

[13] V. Brites, K. Franzreb, J. N. Harvey, S. G. Sayres, M. W. Ross, D. E. Blumling, A. W. C. Jr, M. Hochlaf, Phys. Chem. Chem. Phys. 13 (2011) 15233.

[14] B. O. Roos, in: G. H. F. Diercksen, S. Wilson (Eds.), Methods in Computational Molecular Physics, D. Reidel Publishing, Dordrecht, Netherlands, 1983, p. 161.

[15] B. O. Roos, in: K. P. Lawley (Ed.), Advances in Chemical Physics, volume 69, Wiley Interscience, New York, 1987, p. 339.

[16] B. Brooks, H. F. Schaefer, J. Chem. Phys. 70 (1979) 5092.

[17] B. Brooks, W. Laidig, P. Saxe, N. Handy, H. F. Schaefer, Physica Scripta 21 (1980) 312.

[18] T. H. Dunning, J. Chem. Phys. 90 (1989) 1007.

[19] D. E. Woon, T. H. Dunning, J. Chem. Phys. 98 (1993) 1358.

[20] K. Hirao, Chem. Phys. Lett. 190 (1992) 374.

[21] K. Hirao, Chem. Phys. Lett. 196 (1992) 397.

[22] M. W. Schmidt, K. K. Baldridge, J. A. Boatz, S. T. Elbert, M. S. Gordon, J. H. Jensen, S. Koseki, N. Matsunaga, K. A. Nguyen, S. J. Su, T. L. Windus, M. Dupuis, J. A. Montgomery, J. Comput. Chem. 14 (1993) 1347.

[23] GAMESS-US, version 11 August (R1), 2011.

[24] E. Merzbacher, Quantum Mechanics, Wiley, New York, 1967.

[25] A. Kramida, Yu. Ralchenko, J. Reader, and NIST ASD Team, NIST Atomic Spectra Database (ver. 5.2), [Online]. Available: `http://physics.nist.gov/asd` [2014, November 25]. National Institute of Standards and Technology, Gaithersburg, MD., 2014.

[26] G. Verhaegen, F. E. Stafford, J. Drowart, J. Chem. Phys. 40 (1964) 1622.

[27] C. R. Brazier, L. C. O'Brien, P. F. Bernath, J. Chem. Phys. 91 (1989) 7384.

[28] M. Ebben, M. Drabbels, J. J. ter Meulen, J. Chem. Phys. 95 (1991) 2292.

[29] T. J. Butenhoff, E. A. Rohlfing, J. Chem. Phys. 95 (1991) 3939.

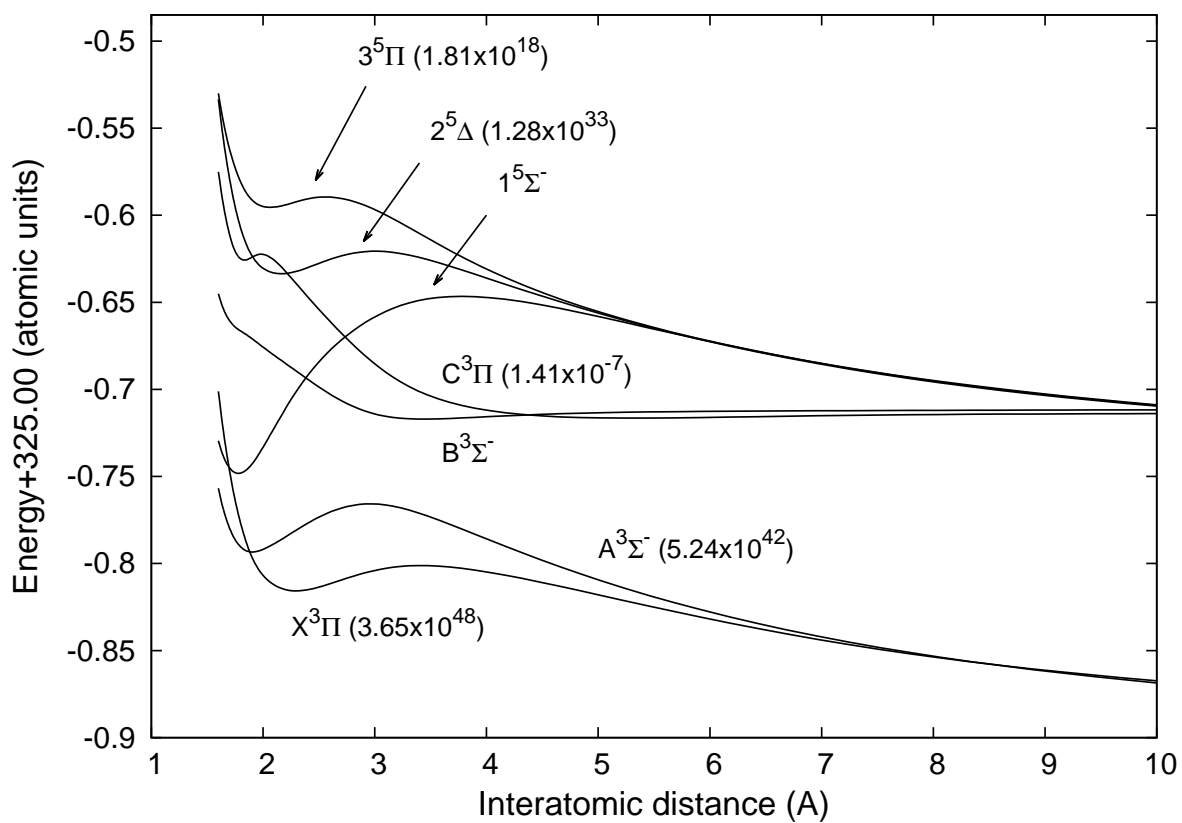Figure 1: Potential energy curves for the lowest-lying triplet and quintet states of SiC^{2+}. Calculated lifetimes, in seconds, are shown in parenthesis for the metastable states.
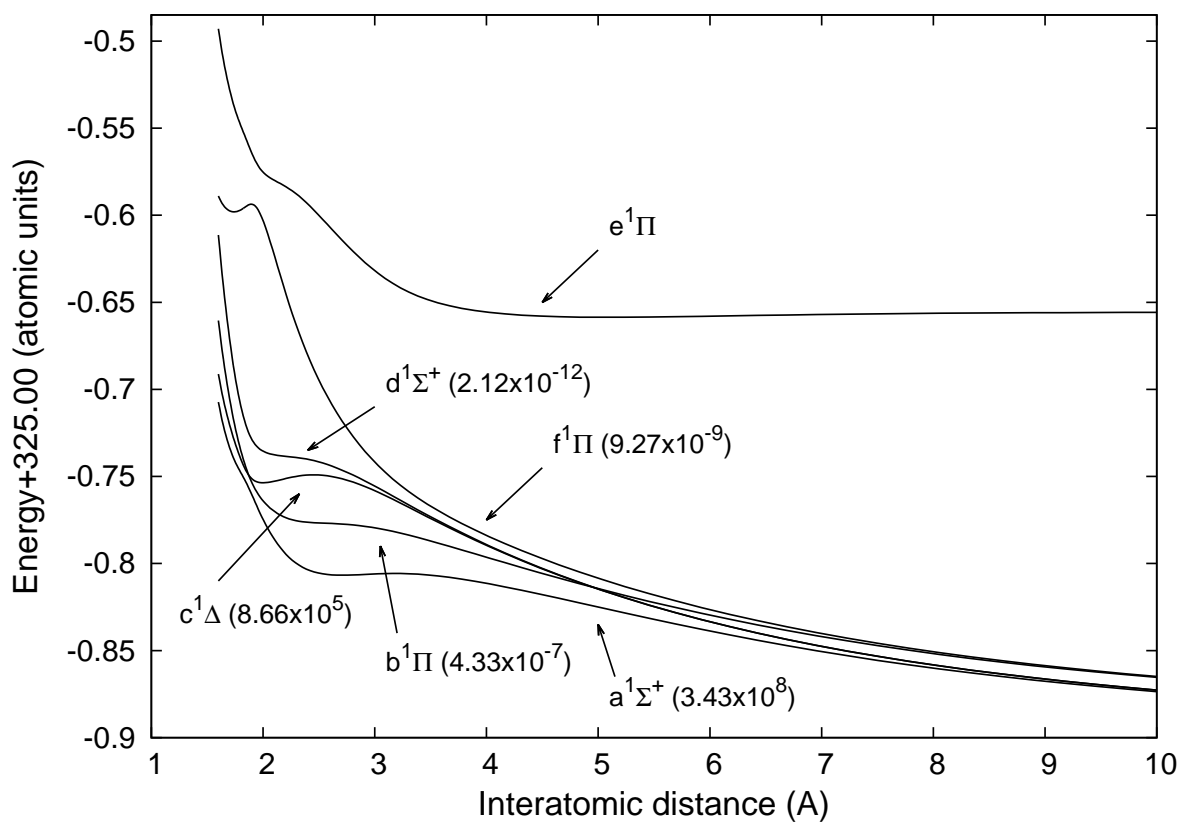
Figure 2: Potential energy curves for the lowest-lying singlet states of SiC^{2+}. Calculated lifetimes, in seconds, are shown in parenthesis for the metastable states.
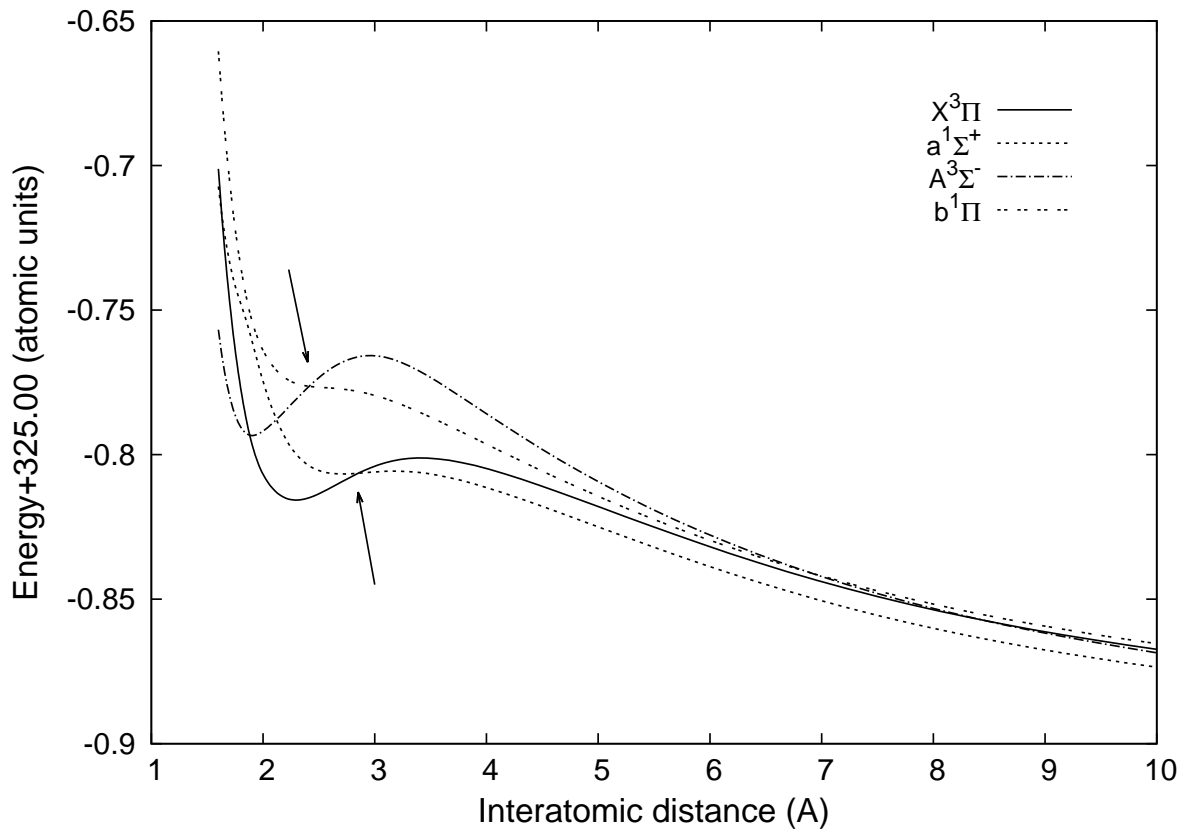
Figure 3: Potential energy curves for the $X^3\Pi$, $A^3\Sigma^-$, $a^1\Sigma^+$ and $b^1\Pi$ metastable states of SiC^{2+}. The crossing points between the $X^3\Pi$ and $a^1\Sigma^+$ states on the one hand and the $A^3\Sigma^-$ and $b^1\Pi$ ones on the other hand are indicated by arrows.

14

Table 1: Properties of low-lying electronic states of neutral SiC. Equilibrium bond distances (R_e in Å) and harmonic frequencies (ω_e in cm^{-1}) are obtained at the CASSCF/aug-cc-pVTZ level of theory. Dissociation energies (D_0 in eV) and energy separations (T_0 in cm^{-1}) are obtained at the MRMP2/aug-cc-pV5Z level of theory.

State	This work				Other works				
	R_e	ω_e	D_0	T_0	R_e	ω_e	D_0	T_e	Reference
X$^3\Pi$	1.749	948	4.32	0.0	1.726	954	4.38	0.0	[5]
					1.74	930		0.0	[6]
					1.7187	965.786			[7]
							4.66		[26]
					1.722[1]				[27]
						964.6			[28]
					1.718	965.16			[29]
A$^3\Sigma^-$	1.839	808	3.81	4138.7	1.811	860	3.90	3883	[5]
					1.82	857		3985	[6]
					1.8001	866.755		3752.14	[7]
					1.814[1]			4578[2]	[27]
a$^1\Sigma^+$	1.675	985	3.68	5148.9	1.656	1023	3.77	6628	[5]
					1.68	975		5325	[6]
					1.6546	1008.45		4830.64	[7]
b$^1\Pi$	1.764	877	3.47	6900.1	1.741	942	3.51	7662.3	[5]
					1.75	930		6725	[6]
					1.7277	944.980		6627.69	[7]
c$^1\Delta$	1.867	787	3.22	8875.2	1.834	814	3.34	8397	[5]
					1.85	790		9135	[6]
					1.8272	821.691		8349.91	[7]
d$^1\Sigma^+$	1.850	890	2.80	12252.5	1.808	979		12603	[5]
					1.84	880		12705	[6]
					1.7993	984.020		12645.47	[7]
1$^5\Pi$	1.960	652	2.47	14923.6	1.942	659	2.39	16095	[5]
					1.97	635		14460	[6]
B$^3\Sigma^+$	1.690	942	1.96	19042.4	1.652	1050	1.94	19658	[5]
					1.68	890		19800	[6]
C$^3\Pi$	1.887	592	1.63	21679.8	1.911	594	1.57	22642	[5]
					1.95	580		21915	[6]
					1.9125	615.122		22894.76	[7]
						618.85		22829[2]	[28]
					1.919	615.72		22830[2]	[7]
e$^1\Sigma^-$	2.198	450	1.32	24232.0	2.130	503	2.10	24703	[5]
					2.18	490		23245	[6]
					2.1205	503.283		24680.14	[7]
D$^3\Delta$	2.192	424	1.21	25059.2	2.133	495	1.22	25489	[5]
					2.18	508		24485	[6]
					2.1156	508.548		25562.65	[7]
E$^3\Pi$	2.021	495	1.90	25405.1	1.929	553	1.80	27080	[5]
					1.94	600		25875	[7]
					1.9149	553.291		26997.57	[7]
F$^3\Sigma^+$	2.128	642	1.14	25689.8	2.025	867	0.95	27644	[5]
					2.0063	916.532		28014.40	[7]

[1] This is reported as R_0.

[2] This is reported as T_0.

Table 2: Leading CSF contributing to the electronic configuration of low-lying electronic states of neutral SiC. CSF were obtained at the MRMP2/aug-cc-pV5Z level of theory.

State	Leading CSF
$X^3\Pi$	$0.92(5\sigma^2 6\sigma^2 7\sigma^1 2\pi^3(\uparrow;\uparrow\downarrow))$
$A^3\Sigma^-$	$0.95(5\sigma^2 6\sigma^2 7\sigma^2 2\pi^2(\uparrow;\uparrow))$
$a^1\Sigma^+$	$0.87(5\sigma^2 6\sigma^2 2\pi^4)$ - $0.22(5\sigma^2 7\sigma^2 2\pi^4)$
$b^1\Pi$	$0.94(5\sigma^2 6\sigma^2 7\sigma^1 2\pi^3(\downarrow;\uparrow\downarrow))$
$c^1\Delta$	$0.67(5\sigma^2 6\sigma^2 7\sigma^2 2\pi^2(\uparrow\downarrow;-))$ - $0.67(5\sigma^2 6\sigma^2 7\sigma^2 2\pi^2(-;\uparrow\downarrow))$
$d^1\Sigma^+$	$0.60(5\sigma^2 6\sigma^2 7\sigma^2 2\pi^2(\uparrow\downarrow;-))$ + $0.60(5\sigma^2 6\sigma^2 7\sigma^2 2\pi^2(-;\uparrow\downarrow))$ + $0.30(5\sigma^2 6\sigma^2 2\pi^4)$ - $0.21(5\sigma^2 7\sigma^2 2\pi^4)$
$1^5\Pi$	$0.95(5\sigma^2 6\sigma^2 7\sigma^1 2\pi^2(\uparrow;\uparrow)3\pi^1(-;\uparrow))$
$B^3\Sigma^+$	$0.73(5\sigma^2 6\sigma^1 7\sigma^1 2\pi^4)$ - $0.35(5\sigma^2 6\sigma^2 2\pi^3(\uparrow\downarrow;\uparrow)3\pi^1(-;\uparrow))$ - $0.35(5\sigma^2 6\sigma^2 2\pi^3(\uparrow;\uparrow\downarrow)3\pi^1(\uparrow;-))$
$C^3\Pi$	$0.49(5\sigma^2 6\sigma^2 7\sigma^1 2\pi^2(-;\uparrow\downarrow)3\pi^1(\uparrow;-))$ + $0.41(5\sigma^2 6\sigma^2 7\sigma^1 2\pi^3(\uparrow;\uparrow\downarrow))$ + $0.40(5\sigma^2 6\sigma^1 7\sigma^2 2\pi^3(\uparrow;\uparrow\downarrow))$ + $0.35(5\sigma^2 6\sigma^2 7\sigma^1 2\pi^2(\uparrow;\downarrow)3\pi^1(-;\uparrow))$ - $0.33(5\sigma^2 6\sigma^2 7\sigma^1 2\pi^2(\uparrow;\uparrow)3\pi^1(-;\downarrow))$
$e^1\Sigma^-$	$0.68(5\sigma^2 6\sigma^2 7\sigma^2 2\pi^1(\uparrow;-)3\pi^1(-;\downarrow))$ - $0.68(5\sigma^2 6\sigma^2 7\sigma^2 2\pi^1(;-\downarrow)3\pi^1(\uparrow;-))$
$D^3\Delta$	$0.68(5\sigma^2 6\sigma^2 7\sigma^2 2\pi^1(\uparrow;-)3\pi^1(-;\uparrow))$ - $0.68(5\sigma^2 6\sigma^2 7\sigma^2 2\pi^1(-;\uparrow)3\pi^1(\uparrow;-))$
$E^3\Pi$	$0.91(5\sigma^2 6\sigma^2 7\sigma^1 2\pi^2(\downarrow;\uparrow)3\pi^1(-;\uparrow)$ + $0.20(5\sigma^2 6\sigma^1 7\sigma^2 2\pi^3(\uparrow;\uparrow\downarrow))$
$F^3\Sigma^+$	$0.59(5\sigma^2 6\sigma^2 7\sigma^2 2\pi^1(\uparrow;-)3\pi^1(\uparrow;-))$ + $0.59(5\sigma^2 6\sigma^2 7\sigma^2 2\pi^1(-;\uparrow)3\pi^1(-;\uparrow))$ + $0.24(5\sigma^2 6\sigma^2 2\pi^3(\uparrow;\uparrow\downarrow)3\pi^1(\uparrow;-))$ + $0.24(5\sigma^2 6\sigma^2 2\pi^3(\uparrow\downarrow;\uparrow)3\pi^1(-;\uparrow))$

Table 3: Properties of low-lying electronic states of SiC$^+$. Equilibrium bond distances (R_e in Å) and harmonic frequencies (ω_e in cm^{-1}) are obtained at the CASSCF/aug-cc-pVTZ level of theory. Dissociation energies (D_0 in eV) and energy separations (T_0 in cm^{-1}) are obtained at the MRMP2/aug-cc-pV5Z level of theory.

State	This work				Reference [8]			
	R_e	ω_e	D_e	T_0	R_e	ω_e	D_0	T_e
X$^4\Sigma^-$	1.830	851	3.62	0.0	1.83	817	3.32	0.0
a$^2\Delta$	1.896	678	2.44	9496.9	1.88	723	2.05	10266
b$^2\Pi$	1.748	830	2.27	10918.1	1.99	480, 700		10696
c$^2\Sigma^-$	1.875	712	2.26	11004.5	1.86	759		11492
d$^2\Sigma^+$	1.885	731	2.06	12572.9	1.91	651		13666
e$^2\Pi$	1.907	1068	1.88	14012.3	1.87	1013		14311
A$^4\Delta$	2.467	293	0.91	21854.6	2.46	285		21173
B$^4\Sigma^+$	2.447	286	0.79	22828.0	2.48	281		21473
C$^4\Pi$	1.706	980	0.73	23300.3				
f$^2\Sigma^-$	2.346	434	0.72	23417.7	2.34	402		23723
g$^2\Pi$-1	2.635	342	0.98[1]					
g$^2\Pi$-2	1.821	500	0.29[2]	30704.3				
h$^2\Sigma^+$	2.418	354	1.01	30902.3	2.45	309		30873
D$^4\Pi$	1.916	842	2.61[3]	34853.8				
1$^6\Pi$	1.856	782	2.08	37177.8				
E$^4\Sigma^+$	4.522	90	1.05	51318.4				
2$^6\Pi$	2.439	347	0.03	59604.3				

[1] Calculated at the CASSCF/aug-cc-pVTZ level of theory as no convergence was achieved at the MRMP2/aug-cc-pV5Z one.

[2] Dissociation energy with respect to the top of the barrier located at 2.200 Å and 0.36 eV above the first minimum, g$^2\Pi$-1.

[3] Metastable state. Dissociation energy with respect to the top of the barrier located at 2.261 Å and 1.63 eV above the dissociation limit.

Table 4: Leading CSF contributing to the electronic configuration of low-lying electronic states of SiC$^+$. CSF were obtained at the MRMP2/aug-cc-pV5Z level of theory.

State	Leading CSF
X$^4\Sigma^-$	$0.93(5\sigma^2 6\sigma^2 7\sigma^1 2\pi^2(\uparrow;\uparrow))$
a$^2\Delta$	$0.81(5\sigma^2 6\sigma^2 7\sigma^1 2\pi^2(\uparrow;\downarrow)) + 0.41(5\sigma^2 6\sigma^2 7\sigma^1 2\pi^2(\downarrow;\uparrow))$
b$^2\Pi$	$0.88(5\sigma^2 6\sigma^2 2\pi^3(\uparrow;\uparrow\downarrow))$
c$^2\Sigma^-$	$0.81(5\sigma^2 6\sigma^2 7\sigma^1 2\pi^2(\downarrow;\uparrow))$ - $0.47(5\sigma^2 6\sigma^2 7\sigma^1 2\pi^2(\uparrow;\downarrow))$
d$^2\Sigma^+$	$0.92(5\sigma^2 6\sigma^2 7\sigma^1 2\pi^2(\uparrow\downarrow;-))$
e$^2\Pi$	$0.68(5\sigma^2 6\sigma^2 7\sigma^2 2\pi^1(\uparrow;-))$ - $0.58(5\sigma^2 6\sigma^2 2\pi^3(\uparrow;\uparrow\downarrow))$
A$^4\Delta$	$0.68\ (5\sigma^2 6\sigma^2 7\sigma^1 2\pi^1(\uparrow;-)3\pi^1(-;\uparrow)$ - $0.68\ (5\sigma^2 6\sigma^2 7\sigma^1 2\pi^1(-;\uparrow)3\pi^1(\uparrow;-))$
B$^4\Sigma^+$	$0.97(5\sigma^2 6\sigma^2 7\sigma^1 2\pi^1(\uparrow;-)3\pi^1(\uparrow;-))$
C$^4\Pi$	$0.87(5\sigma^2 6\sigma^1 7\sigma^1 2\pi^3(\uparrow;\uparrow\downarrow)) + 0.30(5\sigma^2 6\sigma^2 2\pi^2(\uparrow;\uparrow)3\pi^1(-;\uparrow))$
f$^2\Sigma^-$	$0.56(5\sigma^2 6\sigma^2 7\sigma^1 2\pi^1(\uparrow;-)3\pi^1(-;\downarrow))$ - $0.47(5\sigma^2 6\sigma^2 7\sigma^1 2\pi^1(-;\downarrow)3\pi^1(\uparrow;-))$ - $0.37(5\sigma^2 6\sigma^2 7\sigma^1 2\pi^1(-;\uparrow)3\pi^1(\downarrow;-)) + 0.35(5\sigma^2 6\sigma^2 7\sigma^1 2\pi^1(\downarrow;\uparrow))$
g$^2\Pi$-2	$0.55(5\sigma^2 6\sigma^1 7\sigma^1 2\pi^3(\downarrow;\uparrow\downarrow))$ - $0.42(5\sigma^2 6\sigma^2 2\pi^2(-;\uparrow\downarrow)3\pi^1(\uparrow;-))$ - $0.37(5\sigma^2 6\sigma^2 2\pi^2(\uparrow;\downarrow)3\pi^1(-;\uparrow)) + 0.33(5\sigma^2 6\sigma^2 2\pi^2(\uparrow;\uparrow)3\pi^1(-;\downarrow))$
h$^2\Sigma^+$	$0.83(5\sigma^2 6\sigma^2 7\sigma^1 2\pi^1(\downarrow;-)3\pi^1(\uparrow;-))$ - $0.41(5\sigma^2 6\sigma^2 7\sigma^1 2\pi^1(\uparrow;-)3\pi^1(\downarrow;-))$
D$^4\Pi$	$0.70(5\sigma^2 6\sigma^2 2\pi^2(\uparrow;\uparrow)3\pi^1(-;\uparrow)) + 0.54\ (5\sigma^2 6\sigma^1 7\sigma^1 2\pi^3(\uparrow;\uparrow\downarrow))$
1$^6\Pi$	$0.97(5\sigma^2 6\sigma^1 7\sigma^1 2\pi^2(\uparrow;\uparrow)3\pi^1(-;\uparrow))$
E$^4\Sigma^+$	$0.89(5\sigma^2 6\sigma^2 8\sigma^1 2\pi^1(\uparrow;-)3\pi^1(\uparrow;-)) + 0.32\ (5\sigma^2 6\sigma^2 7\sigma^1 2\pi^1(\uparrow;-)3\pi^1(\uparrow;-))$
2$^6\Pi$	$0.67(5\sigma^2 6\sigma^1 7\sigma^1 2\pi^2(\uparrow;\uparrow)3\pi^1(-;\uparrow))$ - $0.46(5\sigma^2 6\sigma^1 7\sigma^1 2\pi^1(-;\uparrow)3\pi^2(\uparrow;\uparrow))$ - $0.45(5\sigma^1 6\sigma^2 7\sigma^1 2\pi^1(-;\uparrow)3\pi^2(\uparrow;\uparrow))$ - $-0.30(5\sigma^1 6\sigma^2 7\sigma^1 2\pi^2(\uparrow;\uparrow)3\pi^1(-;\uparrow))$

Table 5: Properties of low-lying electronic states of SiC^{2+}. Equilibrium bond distances (R_e in Å) and harmonic frequencies (ω_e in cm^{-1}) are obtained at the CASSCF/aug-cc-pVTZ level of theory. Dissociation energies (D_0 in eV), energy separations (T_0 in cm^{-1}) and leading CSF contributing to the electronic configuration are obtained at the MRMP2/aug-cc-pV5Z level of theory.

State	R_e	ω_e	D_0	T_0	Leading CSF
$X^3\Pi$	2.262	427	0.72^1	0.0	$0.93(5\sigma^2 6\sigma^2 7\sigma^1 2\pi^1(\uparrow;-))$
$a^1\Sigma^+$	2.586	248	0.21^1	3931.6	$0.92(5\sigma^2 6\sigma^2 7\sigma^2)$
$A^3\Sigma^-$	1.898	608	0.87^1	5378.7	$0.89(5\sigma^2 6\sigma^2 2\pi^2(\uparrow;\uparrow))$ - $0.21(5\sigma^2 7\sigma^2 2\pi^2(\uparrow;\uparrow))$
$b^1\Pi$	2.309	336	0.17^1	8056.4	$0.94(5\sigma^2 6\sigma^2 7\sigma^1 2\pi^1(\downarrow;-))$
$c^1\Delta$	1.980	466	0.59^1	12398.3	$0.64(5\sigma^2 6\sigma^2 2\pi^2(-;\uparrow\downarrow))$ - $0.64(5\sigma^2 6\sigma^2 2\pi^2(\uparrow\downarrow;-))$
$d^1\Sigma^+$	2.128	364	0.05^1	16932.1	$0.59(5\sigma^2 6\sigma^2 2\pi^2(\uparrow\downarrow;-))$ + $0.59(5\sigma^2 6\sigma^2 2\pi^2(-;\uparrow\downarrow))$ + $0.24(5\sigma^2 6\sigma^2 7\sigma^2)$ - $0.20(5\sigma^2 6\sigma^2 3\pi^2(\uparrow\downarrow;-))$ - $0.20(5\sigma^2 6\sigma^2 3\pi^2(-;\uparrow\downarrow))$
$1^5\Sigma^-$	1.780	896	3.71^1	16940.7	$0.95(5\sigma^2 6\sigma^1 7\sigma^1 2\pi^2(\uparrow;\uparrow))$
$B^3\Sigma^-$	3.158	287	1.14^2	19709.0	$0.97(5\sigma^2 6\sigma^2 2\pi^1 3\pi^1)$ - $0.60(5\sigma^2 6\sigma^2 2\pi^2(\uparrow\uparrow))$
$e^1\Pi$	4.284	119	0.28^2	26623.8	$0.94(5\sigma^2 6\sigma^2 8\sigma^1(\uparrow)3\pi^1(\downarrow;-))$
$C^3\Pi$-1	4.415	90	$0.13^{2,3}$		
$C^3\Pi$-2	1.821	1120	0.47^1	40908.5	$0.75(5\sigma^2 6\sigma^1 2\pi^3(\uparrow;\uparrow\downarrow))$ - $0.38(5\sigma^2 6\sigma^1 7\sigma^2 3\pi^1(\uparrow;-))$ + $0.30(5\sigma^2 6\sigma^2 7\sigma^1 3\pi^1(\uparrow;-))$
$2^5\Delta$	2.149	493	0.74^1	42450.4	$0.69(5\sigma^2 6\sigma^1 7\sigma^1 2\pi^1(\uparrow;-)3\pi^1(\uparrow;-))$ - $0.69(5\sigma^2 6\sigma^1 7\sigma^1 2\pi^1(-;\uparrow)3\pi^1(-;\uparrow))$
$f^1\Pi$	1.741	798	0.47^1	46981.9	$0.94(5\sigma^2 6\sigma^1 2\pi^3(\downarrow;\uparrow\downarrow))$
$3^5\Pi$	2.073	482	0.66^1	51708.0	$0.94(5\sigma^2 6\sigma^1 2\pi^2(\uparrow;\uparrow)3\pi^1(\uparrow;-))$

[1] Dissociation energy with respect to the top of the barrier.

[2] Dissociation energy with respect to the dissociation limit.

[3] Calculated at the CASSCF/aug-cc-pVTZ level of theory as no convergence was achieved at the MRMP2/aug-cc-pV5Z one.

Table 6: Radiative transition dipole moments, in atomic units, between the different stable states of SiC^{2+}. The length form version of the transition dipole moments is shown. The $f^1\Pi$ state is not included in the table due to the fact that no convergence was achieved during the calculation of transition dipole moments for that state.

Singlet states		Triplet states		Quintet states	
$a^1\Sigma^+ \to b^1\Pi$	0.1937	$X^3\Pi \to A^3\Sigma^-$	0.1294	$1^5\Sigma^- \to 2^5\Delta$	0.0
$a^1\Sigma^+ \to c^1\Delta$	0.0	$X^3\Pi \to B^3\Sigma^-$	0.0072	$1^5\Sigma^- \to 3^5\Pi$	0.0991
$a^1\Sigma^+ \to d^1\Sigma^+$	0.0095	$X^3\Pi \to C^3\Pi$	0.7380	$2^5\Delta \to 3^5\Pi$	0.1552
$a^1\Sigma^+ \to e^1\Pi$	0.1636	$A^3\Sigma^- \to B^3\Sigma^-$	0.0039		
$b^1\Pi \to c^1\Delta$	0.1838	$A^3\Sigma^- \to C^3\Pi$	0.0815		
$b^1\Pi \to d^1\Sigma^+$	0.1732	$B^3\Sigma^- \to C^3\Pi$	0.0040		
$b^1\Pi \to e^1\Pi$	0.8226				
$c^1\Delta \to d^1\Sigma^+$	0.0				
$c^1\Delta \to e^1\Pi$	0.0122				
$d^1\Sigma^+ \to e^1\Pi$	0.0158				

Table 7: Adiabatic ionization energies, in eV, to form SiC^+ from neutral SiC, AIE1, and to form SiC^{2+} from SiC^+, AIE2. Electronic states involved in the processes are shown.

$SiC \to SiC^+$	AIE1	$SiC^+ \to SiC^{2+}$	AIE2
$X^3\Pi \to X^4\Sigma^-$	8.80	$X^4\Sigma^- \to X^3\Pi$	17.42
$X^3\Pi \to a^2\Delta$	9.97	$X^4\Sigma^- \to A^3\Sigma^-$	18.09
$X^3\Pi \to b^2\Pi$	10.15	$X^4\Sigma^- \to 1^5\Sigma^-$	19.52
$X^3\Pi \to c^2\Sigma^-$	10.16	$a^2\Delta \to X^3\Pi$	16.25
$A^3\Sigma^- \to X^4\Sigma^-$	8.28	$a^2\Delta \to b^1\Pi$	17.25
$a^1\Sigma^+ \to b^2\Pi$	9.51	$b^2\Pi \to A^3\Sigma^-$	16.74
$b^1\Pi \to a^2\Delta$	9.12	$b^2\Pi \to c^1\Delta$	17.61
$b^1\Pi \to c^2\Sigma^-$	9.31	$b^2\Pi \to d^1\Sigma^+$	18.17
$c^1\Delta \to d^2\Sigma^+$	9.25	$c^2\Sigma^- \to X^3\Pi$	16.06
$1^5\Pi \to X^4\Sigma^-$	6.95	$c^2\Sigma^- \to b^1\Pi$	17.06
		$d^2\Sigma^+ \to X^3\Pi$	15.87
		$d^2\Sigma^+ \to b^1\Pi$	16.87
		$d^2\Sigma^+ \to c^1\Delta$	17.41

The diatomic dication SiC^{2+} in the gas phase
Supplementary Material

Reinaldo Pis Diez[a], Julio A. Alonso[b,c]

[a]*Departamento de Química, CEQUINOR, Centro de Química Inorgánica (CONICET, UNLP), Facultad de Ciencias Exactas, UNLP, CC 962, 1900 La Plata, Argentina.*
[b]*Departamento de Física Teórica, Atómica y Optica, Universidad de Valladolid, E-47011 Valladolid, Spain.*
[c]*Donostia International Physics Center, 20080 San Sebastian, Spain.*

Supplementary Material

Figure S1 shows the mass spectra measured by Franzreb and Williams for prolonged 17 keV ^{16}O$^-$ ion beam bombardment of a silicon carbide (SiC) surface both as semi-logarithmic and linear plots (inset). Some details with respect to the experimental work were provided elsewhere [1, 2].

According to Figure S1, SiC^{2+} is detected at half-integer m/z 20.5 (assigned to ^{29}Si^{12}C^{2+} plus ^{28}Si^{13}C^{2+}). In addition, the two ion signals at integer m/z 20 (shown in the linear inset divided by 20) and at integer m/z 21 are mostly attributed to ^{28}Si^{12}C^{2+} and ^{30}Si^{12}C^{2+} (plus ^{29}Si^{13}C^{2+}), respectively. The expected isotopic abundance of SiC^{2+} at m/z 20 vs. 20.5 vs. 21 is 16.2:1:0.55.

Note that SiO^{2+} is also observed in Figure S1 at integer m/z 22 (^{28}Si^{16}O^{2+}) and at half-integer m/z 22.5 (^{29}Si^{16}O^{2+}). See ref. [3] for a detailed study of gas-phase SiO^{2+}.

The intense ion signals at m/z 16, m/z 17 and m/z 23 are due to ^{16}O$^+$, ^{16}O^{1}H$^+$ and ^{23}Na$^+$, respectively.

References

[1] J. Fiser, K. Franzreb, J. Lorincik, P. Williams, Eur. J. Mass Spectrom. 15 (2009) 315.

[2] T. V. Alves, W. Hermoso, K. Franzreb, F. R. Ornellas, Phys. Chem. Chem. Phys. 13 (2011) 18297.

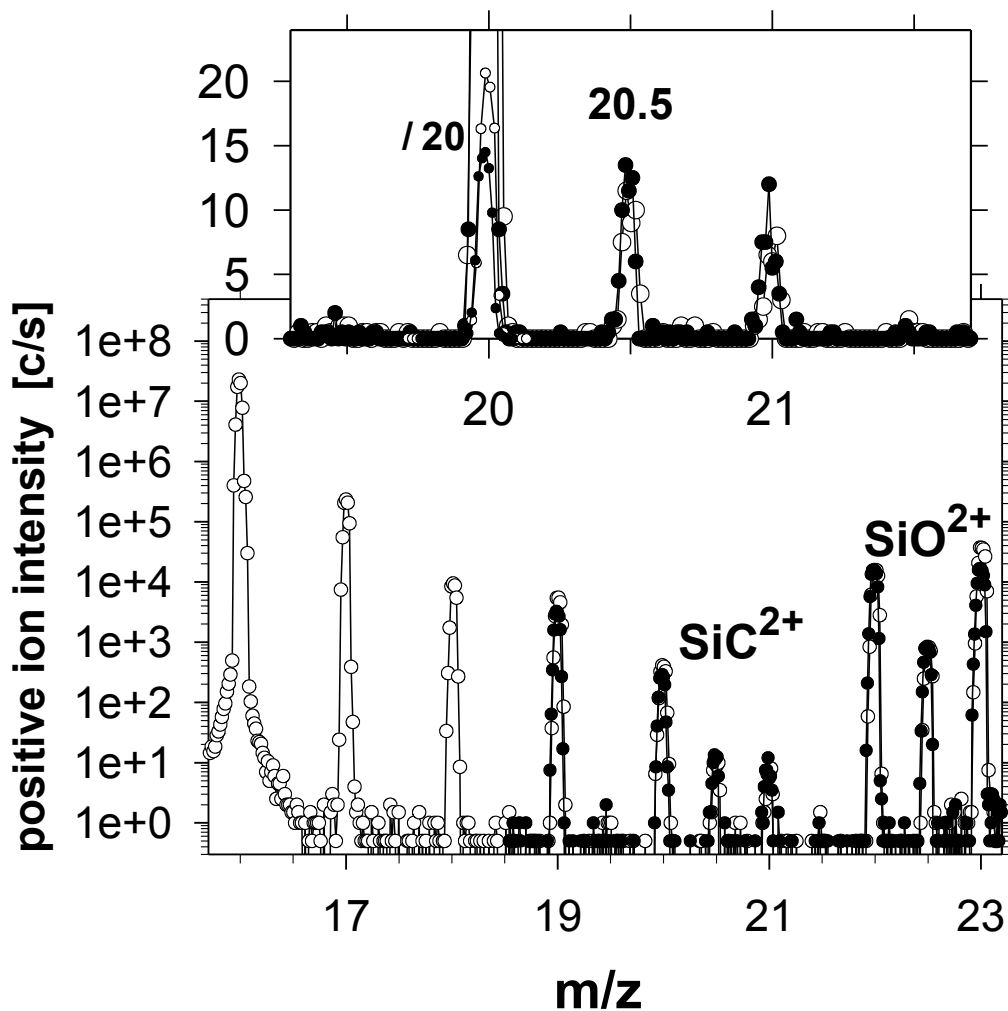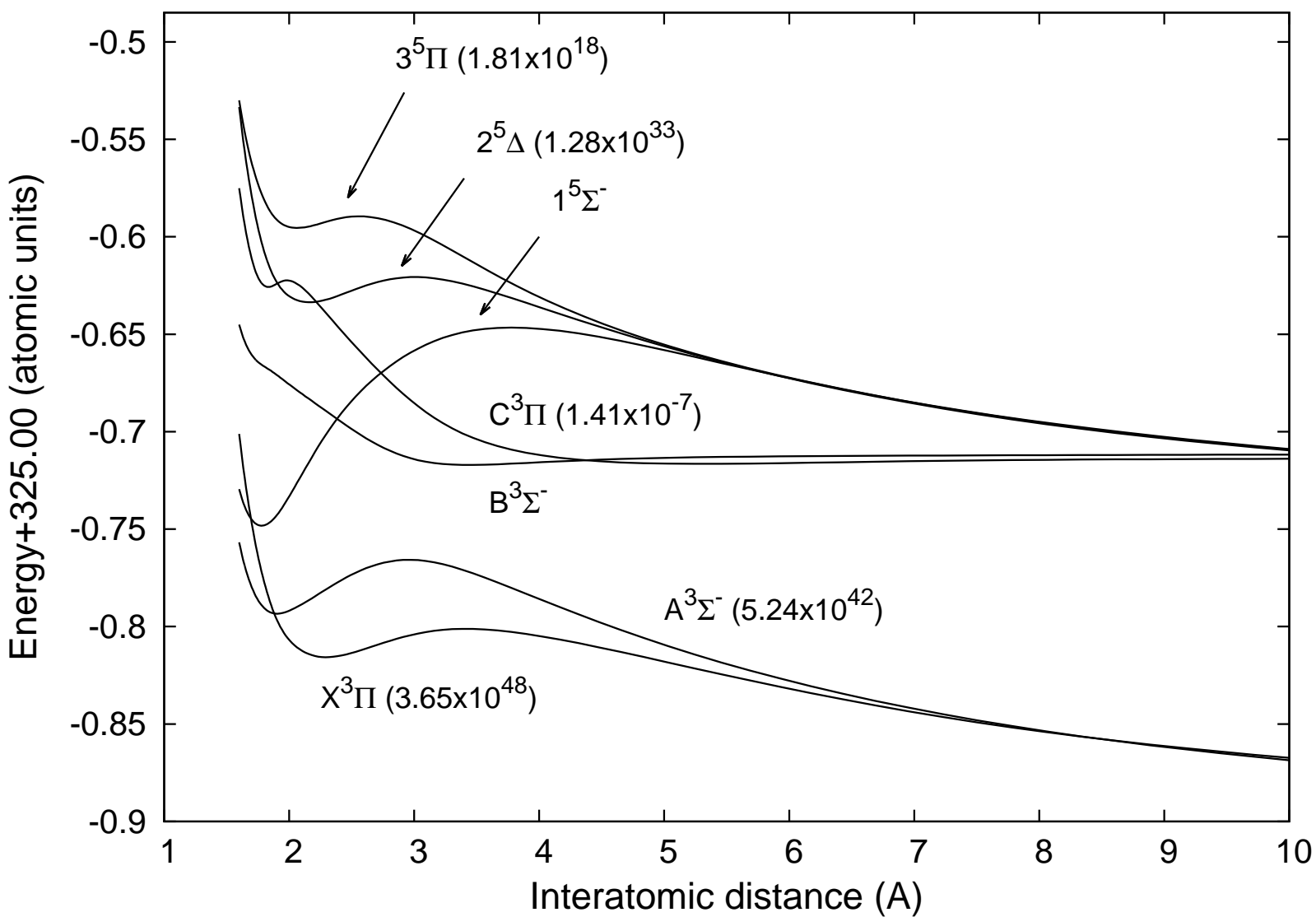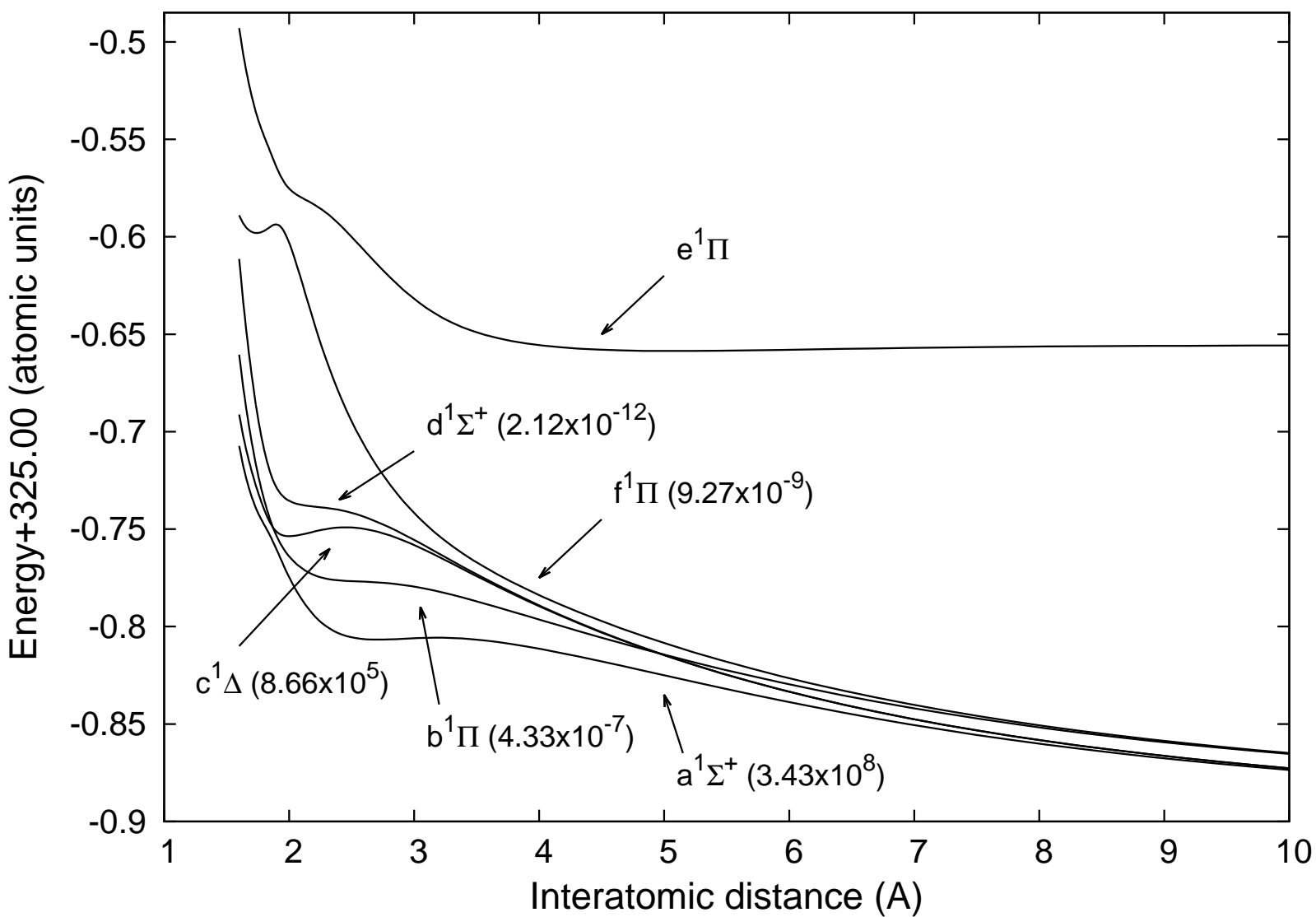[3] S. B. Yaghlane, N. E. Jaidane, K. Franzreb, M. Hochlaf, Chem. Phys. Lett. 486 (2010) 16.

Figure S1: Two positive ion mass spectra of SiC^{2+} acquired for 0.4 μA, 17 keV $^{16}O^{-}$ ion beam sputtering of a piece of a silicon carbide (SiC) wafer. Data is courtesy of Klaus Franzreb and Peter Williams, who used a Cameca IMS 3f magnetic-sector mass spectrometer (sample potential 4500 V, count time 2 s per data point, Arizona State University, 2007, previously unpublished results). See text for a detailed explanation of the meaning of signals.
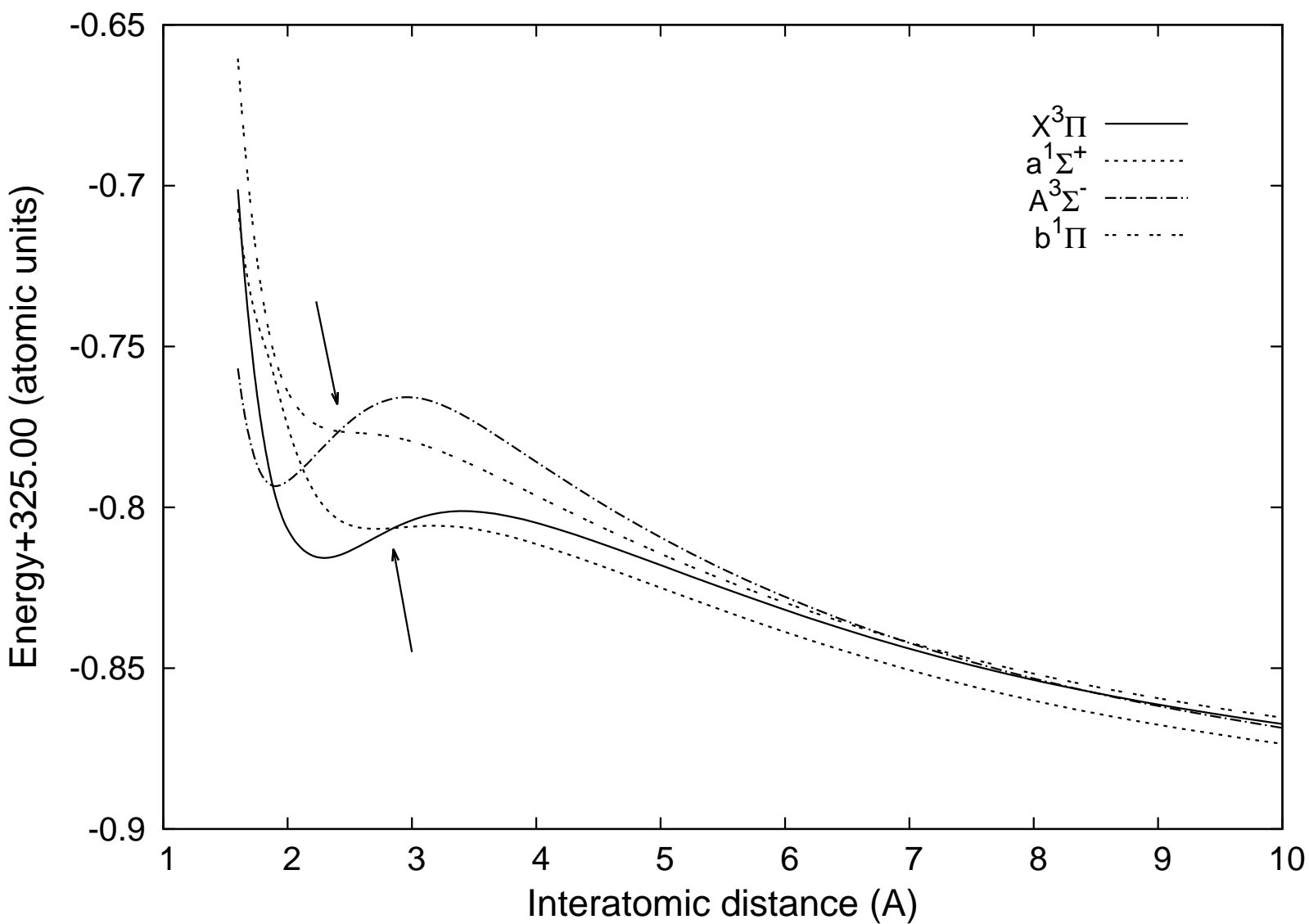
3